First results from GERDA Phase II

IOP Conf. Series: Journal of Physics: Conf. Series **888** (2017) 012030 doi:10.1088/1742-6596/888/1/012030

First results from GERDA Phase II

M Agostini[1,*], M Allardt[4], A M Bakalyarov[13], M Balata[1], I Barabanov[11], L Baudis[19], C Bauer[7], E Bellotti[8,9], S Belogurov[12,11], S T Belyaev[13], G Benato[19], A Bettini[16,17], L Bezrukov[11], T Bode[15], D Borowicz[3,5], V Brudanin[5], R Brugnera[16,17], A Caldwell[14], C Cattadori[9], A Chernogorov[12], V D'Andrea[1], E V Demidova[12], N Di Marco[1], A Domula[4], E Doroshkevich[11], V Egorov[5], R Falkenstein[18], N Frodyma[3], A Gangapshev[11,7], A Garfagnini[16,17], C Gooch[14], P Grabmayr[18], V Gurentsov[11], K Gusev[5,13,15], J Hakenmüller[7], A Hegai[18], M Heisel[7], S Hemmer[17], W Hofmann[7], M Hult[6], L V Inzhechik[11], J Janicskó Csáthy[15], J Jochum[18], M Junker[1], V Kazalov[11], T Kihm[7], I V Kirpichnikov[12], A Kirsch[7], A Kish[19], A Klimenko[7,5], R Kneißl[14], K T Knöpfle[7], O Kochetov[5], V N Kornoukhov[12,11], V V Kuzminov[11], M Laubenstein[1], A Lazzaro[15], V I Lebedev[13], B Lehnert[4], H Y Liao[14], M Lindner[7], I Lippi[17], A Lubashevskiy[7,5], B Lubsandorzhiev[11], G Lutter[6], C Macolino[1], B Majorovits[14], W Maneschg[7], E Medinaceli[16,17], M Miloradovic[19], R Mingazheva[19], M Misiaszek[3], P Moseev[11], I Nemchenok[5], D Palioselitis[14], K Panas[3], L Pandola[2], K Pelczar[3], A Pullia[10], S Riboldi[10], N Rumyantseva[5], C Sada[16,17], F Salamida[9], M Salathe[7], C Schmitt[18], B Schneider[4], S Schönert[15], J Schreiner[7], O Schulz[14], A-K Schütz[18], B Schwingenheuer[7], O Selivanenko[11], E Shevchik[5], M Shirchenko[5], H Simgen[7], A Smolnikov[7,5], L Stanco[17], L Vanhoefer[14], A A Vasenko[12], A Veresnikova[11], K von Sturm[16,17], V Wagner[7], A Wegmann[7], T Wester[4], C Wiesinger[15], M Wojcik[3], E Yanovich[11], I Zhitnikov[5], S V Zhukov[13], D Zinatulina[5], K Zuber[4], G Zuzel[3]

[1]LNGS & GSSI (INFN), [2]LNS (INFN), [3]IoP Cracow, [4]TU Dresden, [5]JINR Dubna, [6]EU Geel, [7]MPI Heidelberg, [8]U. Bicocca Milan, [9]INFN Bicocca Milan, [10]U.d.Studi Milan, [11]INR Moscow, [12]ITEP Moscow, [13]Kurchatov Moscow, [14]MPI Munich, [15]TU Munich, [16]U. Padova, [17]INFN Padova, [18]EKUT Tübingen, [19]U. Zurich, * speaker. Email: gerda-eb@mpi-hd.mpg.de

Abstract. GERDA is designed for a background-free search of ^{76}Ge neutrinoless double-β decay, using bare Ge detectors in liquid Ar. The experiment was upgraded after the successful completion of Phase I to double the target mass and further reduce the background. Newly-designed Ge detectors were installed along with LAr scintillation sensors. Phase II of data-taking started in Dec 2015 with approximately 36 kg of Ge detectors and is currently ongoing. The first results based on 10.8 kg·yr of exposure are presented. The background goal of 10^{-3} cts/(keV·kg·yr) is achieved and a search for neutrinoless double-β decay is performed by combining Phase I and II data. No signal is found and a new limit is set at $T^{0\nu}_{1/2} > 5.3 \cdot 10^{25}$ yr (90% C.L.).

1. Introduction

The GERDA experiment[1] is designed to search for the neutrinoless double-β ($0\nu\beta\beta$) decay of ^{76}Ge into ^{76}Se and two electrons. The detection of a signal would prove that lepton number is not conserved and neutrinos have a Majorana mass component, as predicted by several extensions of the Standard Model.

GERDA uses high-purity Ge detectors made from material enriched in ^{76}Ge to ~87%[2]. If $0\nu\beta\beta$ decays occur, the produced electrons are absorbed within a few millimeters because of the high density and atomic number of Ge. The expected $0\nu\beta\beta$ decay signature is hence a point-like event with a total energy of $Q_{\beta\beta} = 2039$ keV, i.e. the Q-value of the decay. In addition to a high detection efficiency, Ge detectors ensure an excellent energy resolution ($\lesssim 0.2\%$ at $Q_{\beta\beta}$), no intrinsic background, and the possibility of identifying $0\nu\beta\beta$-like events via pulse shape discrimination (PSD)[3].

Current best limits on the $0\nu\beta\beta$ decay half life ($T^{0\nu}_{1/2}$) are above 10^{25} yr, i.e. more then 15 orders of magnitude larger than the age of the universe. Detectors must be efficiently shielded from external background for detecting such a rare process. The innovative approach of GERDA consists of operating the bare detectors in liquid Ar (LAr), which acts as a cooling material, passive shielding against external natural radioactivity and scintillating veto. The cryostat containing 64 m^3 of LAr is immersed in a water tank instrumented with photomultipliers (PMTs) to detect muon Cherenkov light. The experiment is located underground at the Gran Sasso National Laboratory of INFN in Italy.

In the previous phase of data taking (Phase I), ten detectors have been operated for about 1.5 yr at a background level of 10^{-2} cts/(keV$\cdot$ kg$\cdot$ yr). No signal was found and a limit was set at $T^{0\nu}_{1/2} > 2.1 \cdot 10^{25}$ yr (90% C.L.)[1]. The experiment was subsequently upgraded to double the target mass and reduce the background level by a factor of 10, thanks to a new Ge detector geometry and LAr scintillation sensors. A new data taking phase (Phase II) started in Dec 2015. Here we present data collected during the first five months. The envisioned background level and energy resolution have been achieved. A new search for $0\nu\beta\beta$ decay has been performed with a sensitivity doubled compared to our previous analysis. GERDA Phase II will be a background-free experiment througout its planned exposure of 100 kg$\cdot$ yr, eventually reaching the sensitivity to observe a $0\nu\beta\beta$ signal with $T^{0\nu}_{1/2}$ up to 10^{26}yr.

2. Phase II: set-up and concept

The success of Phase II relies upon the deployment of 30 custom-made BEGe-type detectors [4] and of LAr scintillation sensors. Many components of the set-up were also upgraded, including the lock-system used for lowering detectors and LAr scintillation sensors into the cryostat, the read-out electronics, the contacting solution and the detector holders.

The BEGe detectors have a cylindrical shape with a diameter of 7-8 cm and thickness of 3-4 cm. The read-out electrode (1 cm diameter) is created by B implantation on one of the two flat surfaces. The second electrode covers the remaining surface and is produced by Li diffusion, resulting in a $\sim$1 mm surface dead layer. The electrodes are kept at a potential difference of 4 kV to collect the electron-hole pairs generated by energy deposition inside the detector. The BEGe geometry makes it possible to discriminate $0\nu\beta\beta$-like from background events with a simple mono-parametric cut based on the maximum current of an event normalized to its integral (A/E)[5, 6]. This technique is extremely efficient in suppressing the backgrounds that are expected at $Q_{\beta\beta}$: the Compton continuum from γ-rays is reduced by a factor of $\gtrsim$2, degraded surface α-decays by more than a factor of 10, and surface β-decays by up to a factor of 100 [7, 3].

In total thirty BEGe-type (20 kg) and seven coaxial-type detectors (15.8 kg, Phase I-type detectors) are mounted into strings forming a compact array that is lowered in the cryostat together with the LAr scintillation sensors. The sensors are designed to detect scintillation light emitted in a cylindrical volume of 0.5 m diameter and 2.2 m height centered on the array. The lateral surface of the cylinder is covered by 800 m of optical fibers coated with a wavelength shifter and read-out by Si photomultipliers [8]. Sixteen radio-pure PMTs for cryogenic operation are mounted on the top and bottom surfaces. Each detector string is enclosed in a transparent nylon vessel that isolates the LAr volume surrounding the detectors.

PSD and the LAr scintillation veto are complementary techniques able to identify different classes of background events [9]. PSD identifies multiple-site energy depositions inside the Ge material (e.g. multiple Compton scattering) or single-energy depositions on the detector surface (e.g. surface contaminations). LAr scintillation can be produced by all events in which only part of the energy is released in the Ge material (e.g. decays in the material surrounding the detectors). The combination of PSD and LAr veto was found to suppress ^{226}Ra by a factor of 27$\pm$2 and ^{228}Th by a factor of 300$\pm$28 in measurements with calibration sources. It should however be emphasized that the suppression efficiencies strongly depend on the source, its location and the array configuration.

3. Data analysis and background achievements

A blind analysis is performed as in Phase I. Events with energies at $Q_{\beta\beta} \pm 25$ keV are stored and removed from the data flow. The analysis software and procedures are described in Ref. [10, 11].

Data considered in this analysis are from Dec 2015 till May 2016. The average duty cycle is 82%, mostly due to calibrations and hardware adjustments expected in the starting phase. The stability and performance of the Ge detectors are monitored by injecting test pulses at a

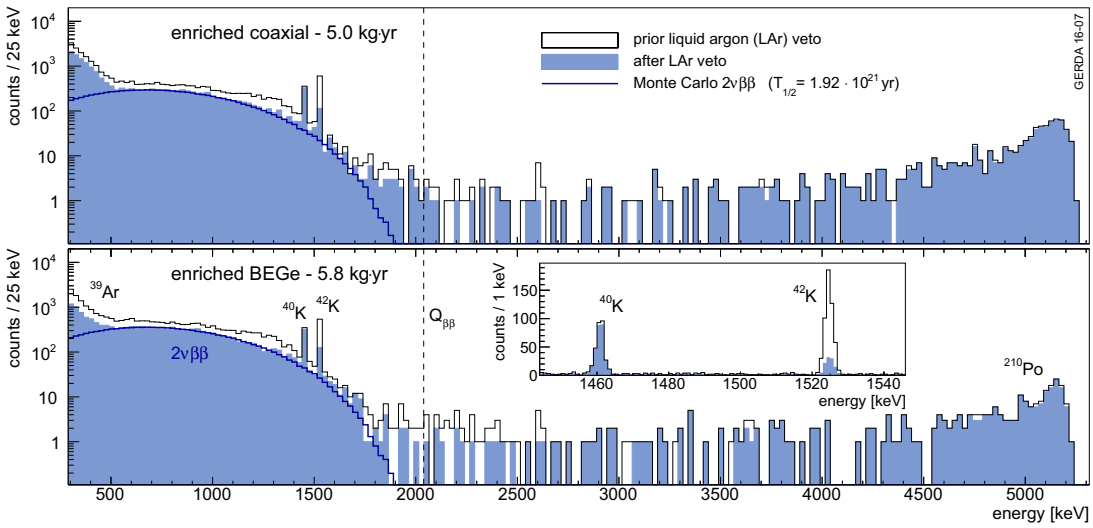

Figure 1. Spectra measured by coaxial and BEGe detectors before and after LAr veto.

50 mHz rate. Only data recorded in stable conditions (e.g. gain stable at 0.1%) are used for physics analysis. This corresponds to about 85% of the total. Signals from electrical discharges or bursts of noise are rejected during the off-line event reconstruction by a set of quality cuts. Genuine signals due to events in the Ge detectors are accepted with an efficiency above 99.9% at $Q_{\beta\beta}$, estimated with artificial samples of simulated events. Data were thoroughly inspected and no hint for unphysical signals was found.

The energy scale and resolution are calibrated weekly by lowering ^{228}Th sources into the cryostat. Uncorrected instabilities of the energy scale are typically smaller than 0.1% at $Q_{\beta\beta}$. Calibrations are also used to optimize the off-line energy reconstruction that is based on a zero area cusp-like filter [12]. The resolution at $Q_{\beta\beta}$ weighted by the exposure of each detector is 4.0 (2) keV for coaxial and 3.0 (2) keV for BEGe detectors.

Events are rejected as background if: a muon trigger is issued within 20 µs; signals are detected simultaneously in multiple detectors; multiple events occur in the same detector within 1 ms. A LAr scintillation veto is issued during the off-line analysis if any of the light detectors record a signal with amplitude >50% of what is expected for a single photoelectron. Events within 5 µs from a LAr veto are rejected. The dead time due to accidental coincidences and the aforementioned cuts is about 3%.

The spectra before and after LAr scintillation veto are shown in Fig 1, separately for coaxial (5.0 kg· yr) and BEGe detectors (5.8 kg· yr). The prominent features are due to the same background components of Phase I [13]: ^{39}Ar cosmogenically produced in LAr (<600 keV); two-neutrino double-β ($2\nu\beta\beta$) decays of ^{76}Ge (600-1700 keV); α-decays on the detector surface, primarily from ^{210}Po (2615-5500 keV). The γ-lines are due to ^{40}K (1464 keV), ^{42}K (1525 keV), ^{214}Bi (1765 keV) and ^{228}Th (2614.5 keV). In spite of the limited statistics of the data set, a comprehensive background model has been developed. The background budget at $Q_{\beta\beta}$ is shared by: the Compton continuum of ^{208}Tl and ^{214}Bi, degraded α-rays from ^{210}Po and β-rays from ^{42}K. This implies that the background at $Q_{\beta\beta}$ is well described by a flat energy distribution.

The performance of the LAr veto are proven by the ^{40}K and ^{42}K γ-lines. The ^{40}K peak survives the veto as the only γ-ray emitted in the EC decay is fully absorbed in the Ge material. Conversely, the ^{42}K peak is suppressed as the γ-ray is emitted in combination with a 2 MeV

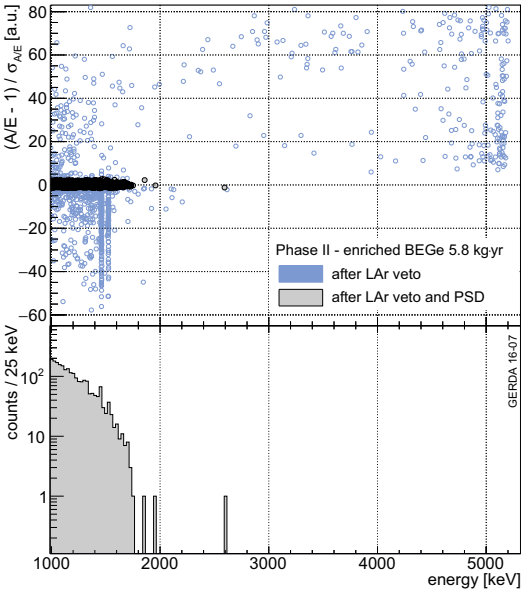

Figure 2. A/E estimator for the events from BEGe detectors. A two-side cut is performed detector-by-detector to select $0\nu\beta\beta$ events and reject backgrounds.

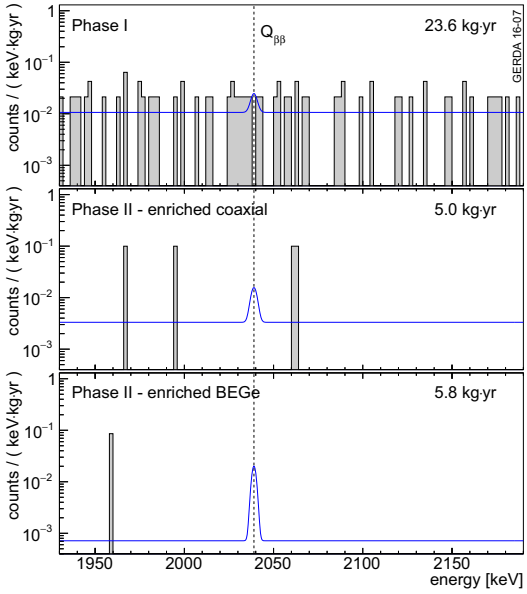

Figure 3. Spectra after analysis cuts. All data sets from Phase I are merged. The blue lines show the fitted background level and the 90% C.L. limits on the $0\nu\beta\beta$ signal strength.

β-ray in LAr. The background reduction at $Q_{\beta\beta}$ is primarily due to the suppression of Compton continuum from ^{208}Tl and ^{214}Bi γ-lines. Similarly, the Compton continuum of ^{40}K and ^{42}K γ-lines is suppressed, leaving basically only $2\nu\beta\beta$ events in the range between 600 and 1300 keV. The background at $Q_{\beta\beta}$ after the LAr veto is $\sim 1\cdot 10^{-2}$ cts/(keV$\cdot$ kg$\cdot$ yr) for coaxial detectors and $\sim 5\cdot 10^{-3}$ cts/(keV$\cdot$ kg$\cdot$ yr) for BEGe detectors. The difference can be related to the rate of α-decays which release all energy in the Ge material and do not produce LAr scintillation.

The background is further reduced by PSD. Fig 2 shows the A/E estimator as a function of the event energy for the BEGe detectors. The central value and resolution of A/E for $0\nu\beta\beta$-like events is detector and energy dependent. After corrections based on calibration data, the distribution of the A/E estimator for $0\nu\beta\beta$-like events becomes approximately Gaussian (centroid of 0, sigma of 1). Background events due to multiple-site energy deposition are reconstructed below $0\nu\beta\beta$-like events, whereas degraded α events are reconstructed above. The PSD results are coherent with our background interpretation and corroborate it. A cut on the A/E estimator is applied separately for each detector. Events with A/E estimator between -1.5 and 3 are on average accepted. The overall survival probability of $0\nu\beta\beta$ events is (87$\pm$2)%, estimated from ^{208}Tl double escaping events.

The PSD technique applied to coaxial detectors is based on two neural networks, designed to discriminate $0\nu\beta\beta$-like events from background multiple-site and degraded α events. The combined survival probability of $0\nu\beta\beta$-like events is (79$\pm$5)%, estimated from simulations and ^{208}Tl double escaping and Compton continuum events. The survival probability of the PSD cuts have been crossed checked against the survival of $2\nu\beta\beta$ events and found to be consistent, both for data from coaxial and BEGe detectors.

The blinded events were eventually processed after fixing all data selection criteria and parameters. Fig 3 shows the final spectra, including all Phase I data (23.6 kg$\cdot$ yr exposure).

Table 1. Parameters of the data sets used for the search of a $0\nu\beta\beta$ signal.

data set		exposure [kg·yr]	signal eff	BI [cts/(keV· kg· yr)]	FWHM [keV]
Phase I	golden	17.9	0.57 (3)	$11 \pm 2 \cdot 10^{-3}$	4.3 (1)
Phase I	silver	1.3	0.57 (3)	$30 \pm 10 \cdot 10^{-3}$	4.3 (1)
Phase I	BEGe	2.4	0.66 (2)	$5^{+4}_{-3} \cdot 10^{-3}$	2.7 (2)
Phase I	extra	1.9	0.58 (4)	$5^{+4}_{-3} \cdot 10^{-3}$	4.2 (2)
Phase II	coaxial	5.0	0.53 (5)	$35^{+21}_{-15} \cdot 10^{-4}$	4.0 (2)
Phase II	BEGe	5.8	0.60 (2)	$7^{+11}_{-5} \cdot 10^{-4}$	3.0 (2)

The background level is computed from a energy region defined prior unblinding: from 1930 to 2190 keV excluding expected γ-lines (2104 ± 5 and 2119 ± 5 keV) and the $0\nu\beta\beta$ decay signal region ($Q_{\beta\beta} \pm 5$ keV). Only one (four) events are found in this region for the data set from BEGe (coaxial) detectors, corresponding to a background level of $7^{+11}_{-5} \cdot 10^{-4}$ cts/(keV· kg· yr) ($35^{+21}_{-15} \cdot 10^{-4}$ cts/(keV· kg· yr)). GERDA has therefore achieved its challenging background goal and it is the first background free experiment of the field. Even considering the final exposure of Phase II, the expected rate for the background in the signal region is less than one count.

4. Search for a $0\nu\beta\beta$ decay signal

A combined analysis of data from Phase I and II is performed, fitting simultaneously the six data sets of Table 1. The number of $0\nu\beta\beta$ events in the i-th data set as a function of $T^{0\nu}_{1/2}$ is:

$$N_i^S(1/T^{0\nu}_{1/2}) = \ln 2 \cdot N_A \cdot \epsilon_i \cdot \eta_i / m_a \cdot (1/T^{0\nu}_{1/2}), \tag{1}$$

where N_A is Avogadro's number, ϵ_i the signal efficiency of the i-th data set, η_i the exposure, and m_a the molar mass of Ge. The exposure quoted is the total detector mass multiplied by the data taking time. The singal efficiencies are the product of: the fraction of ^{76}Ge in the detector material (∼87%), the fraction of detector active volume (∼90%), the efficiency of the analysis cuts (80-90%, dominated by the PSD), and the probability that $0\nu\beta\beta$ decay events in the detector active volume are reconstructed correctly at $Q_{\beta\beta}$ (90-92%). The total number of background events as a function of the background level BI_i is:

$$N_i^B(\mathrm{BI}_i) = \eta_i \cdot \mathrm{BI}_i \cdot \Delta E, \tag{2}$$

where ΔE=240 keV is the energy region used for the fit, i.e. the one used for calculating the background level and extended to the $Q_{\beta\beta}$ region.

Each data set is fitted with an unbinned likelihood function, assuming a Gaussian distribution for the signal and a flat background:

$$\mathcal{L}_i(\mathrm{data}_i|1/T^{0\nu}_{1/2}, \mathrm{BI}_i) = \frac{1}{N_i^S + N_i^B} \prod_{j=0}^{N_i^{obs}} \left[N_i^S \cdot \frac{1}{\sqrt{2\pi}\sigma_i} \cdot \exp\left(\frac{(E_j - Q_{\beta\beta})^2}{\sigma_i^2} \right) + N_i^B \cdot \frac{1}{\Delta E} \right] \tag{3}$$

where the index j runs over all events in a data set, N_i^{obs} is the total number of events observed in the i-th data set, and $\sigma_i = \mathrm{FWHM}_i/(2\sqrt{2\ln 2})$ the energy resolution. The parameters $1/T^{0\nu}_{1/2}$ and BI_i are bounded to positive values. The total likelihood is thus constructed as product of $\mathcal{L}_i$ weighted for the Poissonian extended term [14]:

$$\mathcal{L}(data|1/T^{0\nu}_{1/2}, \mathrm{BI}_i) = \prod_i \left[\mathrm{Poisson}(N_i^{obs}|N_i^S + N_i^B) \cdot \mathcal{L}_i(1/T^{0\nu}_{1/2}, \mathrm{BI}_i) \right] \tag{4}$$

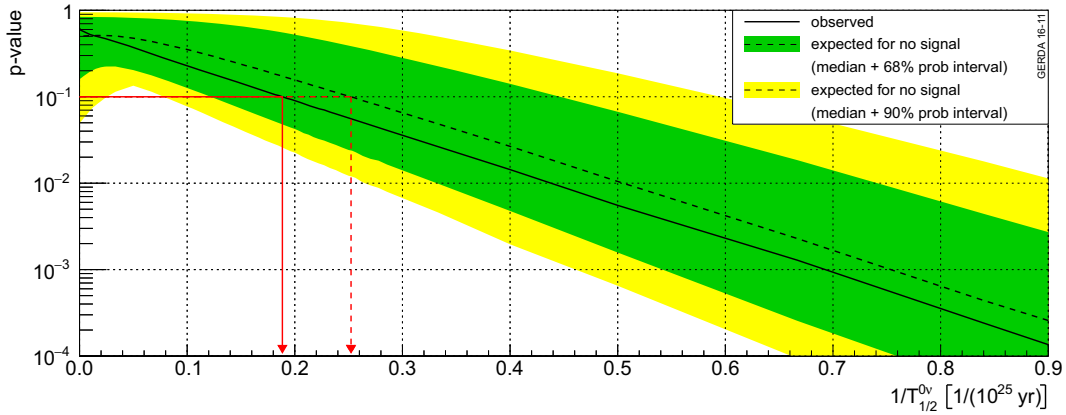

Figure 4. p-value of our data and median p-value expected for no signal (median sensitivity).

Systematics uncertainties on the energy scale, resolution and efficiencies are folded into the analysis as independent Gaussian penalty terms. The pull strength are computed using a Monte Carlo approach which takes correlations into account.

A frequentist analysis is performed with a two-side profile likelihood as test statistic [15]. The distributions of the test statistics as a function of $T^{0\nu}_{1/2}$ are built by a Monte Carlo method. $T^{0\nu}_{1/2}$ values which generate our data with a proabability below 10% are rejected (see Fig 4). The best fit of our data is for no $0\nu\beta\beta$ signal counts and a new limit is set at $T^{0\nu}_{1/2} > 5.3 \cdot 10^{25}$ yr (90% C.L.). The result is close to the median sensitivity expected for no signal: $T^{0\nu}_{1/2} > 4.0 \cdot 10^{25}$ yr (90% C.L.).

In conclusion, the first data from Phase II prove that our detection and shielding concepts work as intended: GERDA will perform a background free search for $0\nu\beta\beta$ decay and increase its sensitivity linearly in time. Within a few years GERDA will reach the sensitivity to detect a signal with $T^{0\nu}_{1/2}$ up to 10^{26} yr.

The GERDA experiment is supported financially by BMBF, DFG, INFN, MPG, NCN, RFBR, and SNF. The institutions acknowledge also internal financial support.

References

[1] Agostini M *et al.* (GERDA) 2013 *Phys. Rev. Lett.* **111** 122503
[2] Ackermann K H *et al.* (GERDA) 2013 *Eur. Phys. J.* **C73** 2330
[3] Agostini M *et al.* (GERDA) 2013 *Eur. Phys. J.* **C73** 2583
[4] Agostini M *et al.* (GERDA) 2015 *Eur. Phys. J.* **C75** 39
[5] Budjas D *et al.* 2009 *JINST* **4** P10007
[6] Agostini M *et al.* 2011 *JINST* **6** P03005
[7] Agostini M 2013 Ph.D. thesis , Munich, Tech. U.
[8] Janicskó-Csáthy J *et al.* 2016 (*Preprint* `arXiv:1606.04254`)
[9] Agostini M *et al.* 2015 *Eur. Phys. J.* **C75** 506
[10] Agostini M *et al.* 2011 *JINST* **6** P08013
[11] Agostini M *et al.* 2012 *J. Phys. Conf. Ser.* **368** 012047
[12] Agostini M *et al.* (GERDA) 2015 *Eur. Phys. J.* **C75** 255
[13] Agostini M *et al.* (GERDA) 2014 *Eur. Phys. J.* **C74** 2764
[14] Beringer J *et al.* (Particle Data Group) 2012 *Phys.Rev.* **D86** 010001
[15] Cowan G *et al.* 2011 *Eur. Phys. J.* **C71** 1554 [Erratum: Eur. Phys. J.C73,2501(2013)]